This document is the accepted manuscript version of the following article:
Sun, Q., Yan, Y., Yao, X., Müllen, K., Narita, A., Fasel, R., & Ruffieux, P. (2021). Evolution of the topological energy band in graphene nanoribbons. Journal of Physical Chemistry Letters, 12(35), 8679-8684.
https://doi.org/10.1021/acs.jpclett.1c02541

Evolution of the Topological Energy Band in Graphene Nanoribbons

Qiang Sun[1,2,], Yuyi Yan[1], Xuelin Yao[3], Klaus Müllen[3], Akimitsu Narita[3,4], Roman Fasel[2,5], and Pascal Ruffieux[2,*]*

[1]Materials Genome Institute, Shanghai University, 200444 Shanghai, China

[2]Empa, Swiss Federal Laboratories for Materials Science and Technology, 8600 Dübendorf, Switzerland

[3]Max Planck Institute for Polymer Research, Ackermannweg 10, 55128 Mainz, Germany

[4]Organic and Carbon Nanomaterials Unit, Okinawa Institute of Science and Technology Graduate University, Okinawa 904-0495, Japan

[5]Department of Chemistry and Biochemistry, University of Bern, 3012 Bern, Switzerland

*Corresponding Author: Pascal.Ruffieux@empa.ch; qiangsun@shu.edu.cn

KEYWORDS: graphene nanoribbon, topological quantum phase, on-surface synthesis, electronic structures, scanning tunneling microscopy, SSH model

TOC Graphic:

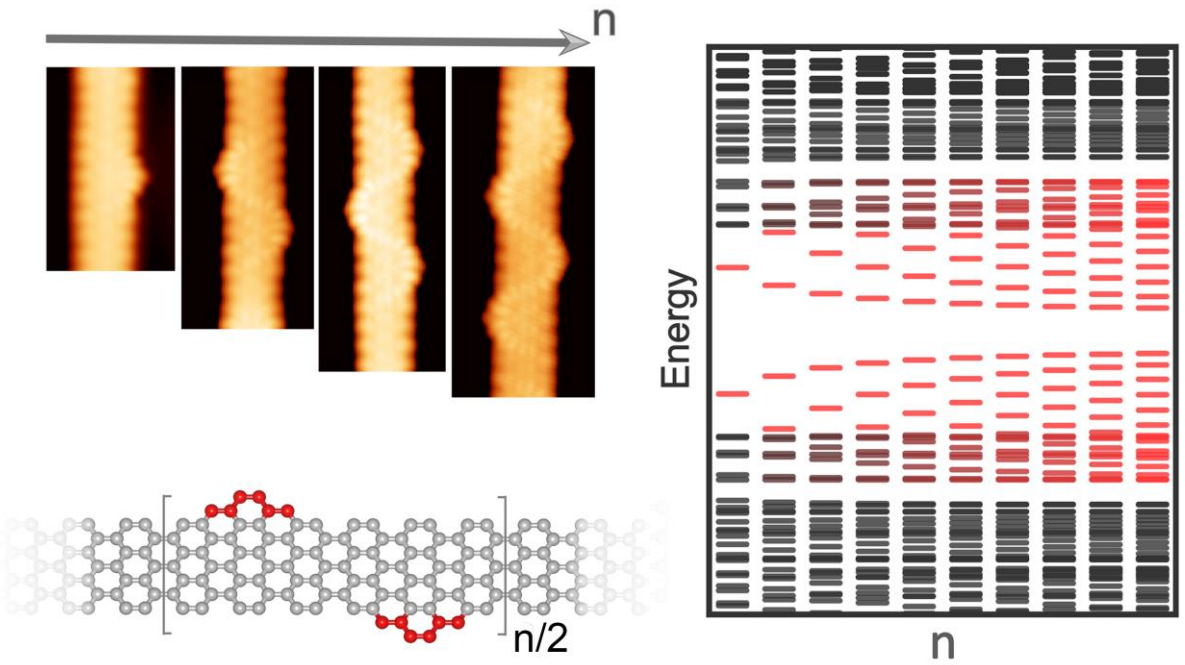

ABSTRACT: Topological theory has been recently applied in graphene nanoribbons (GNRs), and predicts the existence of topological quantum states in junctions connecting GNRs of different topological classes. Through the periodic alignment of the topological states along a GNR backbone, frontier GNR electronic bands with tunable band gaps and band widths could be generated. In this work, we demonstrate the evolution of the topological band by fabricating GNR structures hosting single topological junction, dimerized junctions and multiple coupled junctions with on-surface synthesis, which guarantees the atomic precision of these

nanostructures. Their structural and electronic properties are investigated by scanning tunneling microscopy and spectroscopy supported by tight-binding theory. The 1D superlattice of the topological junction states can be described by an effective two-band tight-binding Su-Schrieffer-Heeger (SSH) type model considering two alternating coupling motifs.

Topological concepts have gained considerable attention in materials science and provide deep insights to novel physical phenomena such as the quantum Hall effect, topological insulator and other quantum phases of matter.[1-5] One of the characteristics of topological materials is the in-gap state at the boundary of two connecting insulators with different topological classes.[6, 7] Although most work has been concentrating on three-dimensional or two-dimensional materials, recent advances in the fabrication of atomically precise graphene nanoribbons (GNRs) have also motivated the theoretical demonstration of one-dimensional symmetry-protected topological phase in GNRs, which predicts that the semiconducting armchair edged GNRs (AGNRs) with different widths and unit cell termini belong to different electronic topological phases.[8] Later on, the symmetry-protected topological classification has been extended to more GNRs including cove-edged and chevron-type GNRs which are structurally more diverse.[9, 10] The idea of topological GNR immediately found its application in band engineering of GNRs through the periodic arrangement of topological boundary states along the GNR backbone.[11, 12] A superlattice of such boundary states constructed by connecting two GNR segments of different topological classes will hybridize and result in new frontier bands, thus leading to the topological band engineering. It would therefore be interesting to experimentally demonstrate the formation the topologically derived bands by coupling two and more boundary states, which is however missing.

By the rational design of molecular precursors and the catalytic surfaces, a large number of GNRs with atomic scale control on their edges, widths and chemical compositions are realized

through surface assisted reactions.[13-19] In this work, we focus on a seven-carbon-atom wide armchair GNR with staggered edge extensions (7-AGNR-S(1,3)), chemical structure displayed in Fig. 1e) which was recently demonstrated to have topological bands originating from the 1D superlattice of topological junctions along the longitudinal GNR axis.[11] We have experimentally demonstrated the evolution of the topological band of 7-AGNR-S(1,3) by probing GNRs having single topological junction to those having dimerized junctions, then those with multiple coupled junctions. The 1D superlattice of the topological junction states can be described by an effective two-band tight-binding model consisting of two alternating coupling motifs. The required atomic precision in those structures is achieved through the surface-assisted debromination and cyclodehydrogenation of two molecular precursors under ultra-high vacuum (UHV) conditions. The structural and electronic properties of the nanostructures are characterized by scanning tunneling microscopy and spectroscopy supported by tight-binding calculations.

7-AGNR-S(1,3) can be effectively described by a superlattice of single-sided edge extension with extra benzene rings fused on the 7AGNR backbone (structure I in Fig. 1b represents one of such edge extensions with a naphtha group highlighted by yellow shadows). The edge extension is indeed the junction connecting two GNR segments of different topological classes, [11] which can be rationalized using chiral symmetry.[20] Thus, a topological zero-energy state that can serve as the fundamental building block for new bands (energy spectrum in Fig. 1a) is produced.[21] Further changing the number of fused benzene ring as well as their orientations, two different coupling motifs are constructed, structure II fused with the phenanthro group (highlighted by green shadows) and structure III with two naphtho groups oppositely arranged along the edge of 7AGNR, as shown in Fig. 1b. In both cases, the wave function overlapping between the topological zero-energy states yields two hybridized states, i.e., bonding and antibonding states (energy spectra in Fig. 1a). Since the two states are within the gap of the

pristine 7AGNR, they also represent the highest occupied molecular orbital (HOMO) and lowest unoccupied molecular orbital (LUMO). The two different geometries of edge extensions (structure II and III) lead to two different coupling strengths, which can be reflected by the different gaps in their energy spectra. Through the further fusing the edge extensions along the 7AGNR backbone, more hybridized energy states appear and the resulting frontier energy gaps get smaller (cf. the TB calculated energy spectra in Fig. 1d). In the limit of an infinite number of edge extensions, that is 7-AGNR-S(1,3), dispersive bands deriving from the hybridized state are formed, which stand for the topological bands (the band structure of 7-AGNR-S(1,3) shown in Fig. 1e). This is much like the band formation of electrons in a periodic potential. Here, the periodicity of the effective potential is imposed by the periodic alignment of the edge extensions.

The topological bands arising from the coupled topological states can be expressed by the 1D Su-Schrieffer-Heeger (SSH) model in the standard two-band tight-binding form, which captures the relevant fundamental parameters.[11, 12] The SSH band dispersion follows:

$$E_{\pm}(k) = \pm\sqrt{t_1^2 + t_2^2 + 2t_1 t_2 \cos(k)} \quad (1)$$

Which leads to a tunable energy gap $E_g = 2\big||t_1| - |t_2|\big|$ (2). The two different coupling strengths between the topological states are expressed as hopping amplitudes t_1 (structure II) and t_2 (structure III), and t_1 equals to $E_g/2$ and t_2 equals to $E_g/2$, where E_g denotes the energy gap. Consequently, t_1 and t_2 are determined to be 0.40 and 0.28 eV, respectively from the TB calculated energy spectra of structure II and III. For comparison, we have performed TB calculations of the band structure of 7-AGNR-S(1,3). The topological derived bands are colored in red, and the energy gap equals to 0.12 eV, which nicely matched with the gap value determined from the SSH model capturing the t_1 and t_2 from the coupled topological states and equations (2). These analyses highlight the role of the coupling states in the topological band engineering of the topological GNRs.

Experimentally, we have applied the bottom-up method to realize the atomically precise GNR structures.[22, 23] The structure I which has a single-sided zigzag edge has been demonstrated in our previous work, clearly revealing a topological junction state.[21] To fabricate structure II, we have employed two molecular precursors **1** and **2** (chemical structures shown in Fig. 2a), the synthetic details of which have been previously reported[11, 24]. We have firstly co-deposited precursors **1** and **2** onto the Au (111) surface with an estimated molecular coverage ratio of 1 : 6 so that isolated edge extensions of structure II can be easily observed (see overview STM images of the samples with different molecular coverages between **1** and **2** in **Fig. S1**). The synthesis of the designed edge-extended GNR structure was accomplished by the standard two-step annealing process, i.e., 200 °C to induce the homolytic cleavage of the C-Br bond and C-C coupling, and 350 °C to promote the oxidative cyclization.[25, 26] A typical STM image of the fabricated structure II is displayed in Fig. 2b where we could clearly see the edge extension with the phenanthrene substructure, forming two zigzag edges.

The electronic properties of the structure II were studied by dI/dV scanning tunneling spectroscopy (STS). A typical dI/dV spectrum obtained on the edge extension is shown in Fig. 2c, from which two prominent peaks are clearly resolved with the peak bias at -510 mV and 950 mV, respectively. The two peaks are inside the band gap of 7AGNR on Au(111) (the valence and conduction band onsets of 7AGNR on Au(111) are -0.7 V and 1.6 V, respetively[27]). From a comparison to the TB calculated energy spectrum of the structure II (Fig. 2d), the two peaks can be assigned to the HOMO and LUMO resulting from the hybridization between two topological junction states originating from the single-sided zigzag edges. The spatial distributions of the two hybridized states, i.e., the local density of states (LDOS), were revealed by acquiring the STS maps of the structure II at the peak biases (Fig. 2e). We have also simulated the LDOS maps of the HOMO and LUMO by TB (Fig. 2f), both of which are in excellent agreement with the experimental maps.

To realize structure III, precursor molecule **3** was employed[21]. By mixing molecule **3** with molecule **2** followed by the thermal annealing to 350 °C**,** both the isolated single-sided zigzag edge extension (structure I) and the coupled one (structure III) could be synthesized (Fig. 3a).[21] Fig. 3b displays a standard STM image of the structure III, where two single-sided zigzag edge extensions can be identified. The dI/dV spectrum was then taken above the structure III and two prominent peaks are also resolved at bias of -270 mV and 1050 mV, respectively. From a comparison to the TB calculated energy spectrum of the structure III (Fig. 3d), the two peaks can be attributed to the HOMO and LUMO derived from the hybridization between the two topological states. We have also performed the STS maps at two peak biases and examined the LDOS of the two states (Fig. 3e). The TB simulated LDOS maps of the hybridized states are computed and displayed in Fig. 3f. By comparing the nodal patterns and density distributions, we find a perfect match between the experimental and theoretical maps. Consequently, the two elementary couplings in the formation of the 1D topological GNR bands can be revealed. We note that the coupling strengths of structure II (t_1) is theoretically larger than that of structure III (t_2), which is consistent with the larger experimentally determined hybridized gap for structure II.

After establishing two elementary coupling motifs of the effective SSH model for the topological bands, further coupling of the topological states was achieved via the incorporation of more edge extensions. Experimentally, we increased the relative molecular coverage of precursor **1** with respect to precursor **2** to obtain the GNR structures with additional edge extensions. A number of structures were observed by STM imaging, and investigated by STS spectrum to reveal their electronic properties (see Fig. 4a and Fig. S2 to S4). As predicted by theory (Fig. 1d), more hybridized states appear as a result of the coupling of the edge extensions, and the topological state derived energy gap decreases as a function of the number of coupled

edge extensions. Consequently, the dispersive bands are gradually developed from the hybridized state.

The STS spectra on a series of GNR structures with different numbers of edge extensions are displayed in Fig. 4b, where we clearly see the shrinking of HOMO-LUMO gaps as a function of the number of edge extensions. In Fig. 4c, we summarized the HOMO-LUMO gaps of structures II, structure III and GNR structures with more coupled edge extensions. For comparison, the band gap of the 7-AGNR-S(1,3) which can be expressed as the 7AGNR structure fused with an infinite number of edge extensions is also shown in Fig. 4c, where we see a clear convergence of the HOMO-LUMO gap to the topological band gap as predicted by our theory (Fig. 1c-1e). We note that the discrete energy states of the multiple coupled edge extensions are not resolved in our STS spectra, which is due to the hybridization and broadening of molecular orbitals on metal surfaces. Nevertheless, the discernible frontier energy gap convergence of GNRs with multiple coupled edge extensions unambiguously demonstrates the evolution of the topological band.

In conclusion, we have studied a GNR with topologically derived frontier energy bands. The topological bands originate from the 1D superlattice of topological junctions along the longitudinal GNR axis. By constructing GNR structures with different numbers of topological junctions along a GNR backbone via on-surface synthesis method, we showed the evolution of the topological band from the pristine GNR backbone. Two elementary dimer structures of the topological junctions are fabricated and investigated by our STM measurements combined with TB calculations. Both of them exhibit two in-gap states originating from the hybridization of the topological states. By experimentally aligning multiple edge extensions, i.e., coupling more topological junction states, we reveal the convergence of the HOMO-LUMO gap to the topological band gap, which corroborates the evolution of the topological band. This work rationalizes the topological bands in the zigzag edge extended GNR, and may inspire the

fabrication of novel GNRs with tunable and intriguing band structures. Moreover, this kind of in-gap topological states created by the coupled topological states along the 1D structure may have potential in optoelectronic applications.[28, 29]

Supporting information

The Supporting Information is available free of charge at charge at https://pubs.acs.org/ STM images and STS maps of structure II (n=2,3,4), wave functions of the frontier states for structure II (n=1), experimental and theoretical methods.

Acknowledgements

We thank O. Groning for fruitful discussions. This work was supported by the Swiss National Science Foundation under Grant No. 200020_182015 and No. 200021_172527. We are also grateful for the financial support from the Max Planck Society.

Competing financial interests

The authors declare no competing financial interests.

References:

1. Kane, C. L.; Mele, E. J., Z2 topological order and the quantum spin Hall effect. *Phys Rev Lett* **2005,** *95* (14), 146802.
2. Niemi, A. J.; Semenoff, G. W., Fermion number fractionization in quantum field theory. *Physics Reports* **1986,** *135* (3), 99-193.
3. Fu, L., Topological crystalline insulators. *Phys Rev Lett* **2011,** *106* (10), 106802.
4. Shiozaki, K.; Sato, M., Topology of crystalline insulators and superconductors. *Physical Review B* **2014,** *90* (16).
5. Armitage, N. P.; Mele, E. J.; Vishwanath, A., Weyl and Dirac semimetals in three-dimensional solids. *Reviews of Modern Physics* **2018,** *90* (1).

6. Hasan, M. Z.; Kane, C. L., Colloquium: Topological insulators. *Reviews of Modern Physics* **2010,** *82* (4), 3045-3067.
7. Fu, L.; Kane, C. L., Topological insulators with inversion symmetry. *Physical Review B* **2007,** *76* (4).
8. Cao, T.; Zhao, F.; Louie, S. G., Topological Phases in Graphene Nanoribbons: Junction States, Spin Centers, and Quantum Spin Chains. *Phys Rev Lett* **2017,** *119* (7), 076401.
9. Lin, K.-S.; Chou, M.-Y., Topological Properties of Gapped Graphene Nanoribbons with Spatial Symmetries. *Nano Letters* **2018,** *18* (11), 7254-7260.
10. Lee, Y.-L.; Zhao, F.; Cao, T.; Ihm, J.; Louie, S. G., Topological Phases in Cove-Edged and Chevron Graphene Nanoribbons: Geometric Structures, Z2 Invariants, and Junction States. *Nano Letters* **2018,** *18* (11), 7247-7253.
11. Groning, O.; Wang, S.; Yao, X.; Pignedoli, C. A.; Borin Barin, G.; Daniels, C.; Cupo, A.; Meunier, V.; Feng, X.; Narita, A.; et al, Engineering of robust topological quantum phases in graphene nanoribbons. *Nature* **2018,** *560* (7717), 209-213.
12. Rizzo, D. J.; Veber, G.; Cao, T.; Bronner, C.; Chen, T.; Zhao, F.; Rodriguez, H.; Louie, S. G.; Crommie, M. F.; Fischer, F. R., Topological band engineering of graphene nanoribbons. *Nature* **2018,** *560* (7717), 204-208.
13. Ruffieux, P.; Wang, S.; Yang, B.; Sanchez-Sanchez, C.; Liu, J.; Dienel, T.; Talirz, L.; Shinde, P.; Pignedoli, C. A.; Passerone, D.; et al, On-surface synthesis of graphene nanoribbons with zigzag edge topology. *Nature* **2016,** *531* (7595), 489-92.
14. Cai, J.; Pignedoli, C. A.; Talirz, L.; Ruffieux, P.; Sode, H.; Liang, L.; Meunier, V.; Berger, R.; Li, R.; Feng, X.; et al, Graphene nanoribbon heterojunctions. *Nat Nanotechnol* **2014,** *9* (11), 896-900.
15. Wang, S.; Kharche, N.; Costa Girão, E.; Feng, X.; Müllen, K.; Meunier, V.; Fasel, R.; Ruffieux, P., Quantum Dots in Graphene Nanoribbons. *Nano Letters* **2017,** *17* (7), 4277-4283.
16. Zuzak, R.; Brandimarte, P.; Olszowski, P.; Izydorczyk, I.; Markoulides, M.; Such, B.; Kolmer, M.; Szymonski, M.; Garcia-Lekue, A.; Sanchez-Portal, D.; et al, On-Surface Synthesis of Chlorinated

Narrow Graphene Nanoribbon Organometallic Hybrids. *J Phys Chem Lett* **2020,** *11* (24), 10290-10297.

17. Wang, S.; Talirz, L.; Pignedoli, C. A.; Feng, X.; Mullen, K.; Fasel, R.; Ruffieux, P., Giant edge state splitting at atomically precise graphene zigzag edges. *Nat Commun* **2016,** *7*, 11507.
18. Lawrence, J.; Brandimarte, P.; Berdonces-Layunta, A.; Mohammed, M. S. G.; Grewal, A.; Leon, C. C.; Sanchez-Portal, D.; de Oteyza, D. G., Probing the Magnetism of Topological End States in 5-Armchair Graphene Nanoribbons. *ACS Nano* **2020,** *14* (4), 4499-4508.
19. Li, J.; Sanz, S.; Corso, M.; Choi, D. J.; Pena, D.; Frederiksen, T.; Pascual, J. I., Single spin localization and manipulation in graphene open-shell nanostructures. *Nat Commun* **2019,** *10* (1), 200.
20. Jiang, J.; Louie, S. G., Topology Classification using Chiral Symmetry and Spin Correlations in Graphene Nanoribbons. *Nano Lett* **2021,** *21* (1), 197-202.
21. Sun, Q.; Yao, X.; Groning, O.; Eimre, K.; Pignedoli, C. A.; Mullen, K.; Narita, A.; Fasel, R.; Ruffieux, P., Coupled Spin States in Armchair Graphene Nanoribbons with Asymmetric Zigzag Edge Extensions. *Nano Lett* **2020,** *20* (9), 6429-6436.
22. Sun, Q.; Zhang, R.; Qiu, J.; Liu, R.; Xu, W., On-Surface Synthesis of Carbon Nanostructures. *Adv Mater* **2018,** *30* (17), e1705630.
23. Clair, S.; de Oteyza, D. G., Controlling a Chemical Coupling Reaction on a Surface: Tools and Strategies for On-Surface Synthesis. *Chem Rev* **2019,** *119* (7), 4717-4776.
24. Cai, J.; Ruffieux, P.; Jaafar, R.; Bieri, M.; Braun, T.; Blankenburg, S.; Muoth, M.; Seitsonen, A. P.; Saleh, M.; Feng, X.; et al, Atomically precise bottom-up fabrication of graphene nanoribbons. *Nature* **2010,** *466* (7305), 470-3.
25. Grill, L.; Dyer, M.; Lafferentz, L.; Persson, M.; Peters, M. V.; Hecht, S., Nano-architectures by covalent assembly of molecular building blocks. *Nat Nanotechnol* **2007,** *2* (11), 687-91.
26. Treier, M.; Pignedoli, C. A.; Laino, T.; Rieger, R.; Mullen, K.; Passerone, D.; Fasel, R., Surface-assisted cyclodehydrogenation provides a synthetic route towards easily processable and chemically tailored nanographenes. *Nat Chem* **2011,** *3* (1), 61-7.

27. Ruffieux, P.; Cai, J.; Plumb, N. C.; Patthey, L.; Prezzi, D.; Ferretti, A.; Molinari, E.; Feng, X.; Müllen, K.; Pignedoli, C. A.; et al, Electronic Structure of Atomically Precise Graphene Nanoribbons. *ACS Nano* **2012,** *6* (8), 6930-6935.
28. Ma, C.; Xiao, Z.; Puretzky, A. A.; Wang, H.; Mohsin, A.; Huang, J.; Liang, L.; Luo, Y.; Lawrie, B. J.; Gu, G.; et al, Engineering Edge States of Graphene Nanoribbons for Narrow-Band Photoluminescence. *ACS Nano* **2020,** *14* (4), 5090-5098.
29. Wu, X.; Wang, R.; Liu, N.; Zou, H.; Shao, B.; Shao, L.; Yam, C., Controlling the emission frequency of graphene nanoribbon emitters based on spatially excited topological boundary states. *Phys Chem Chem Phys* **2020,** *22* (16), 8277-8283.

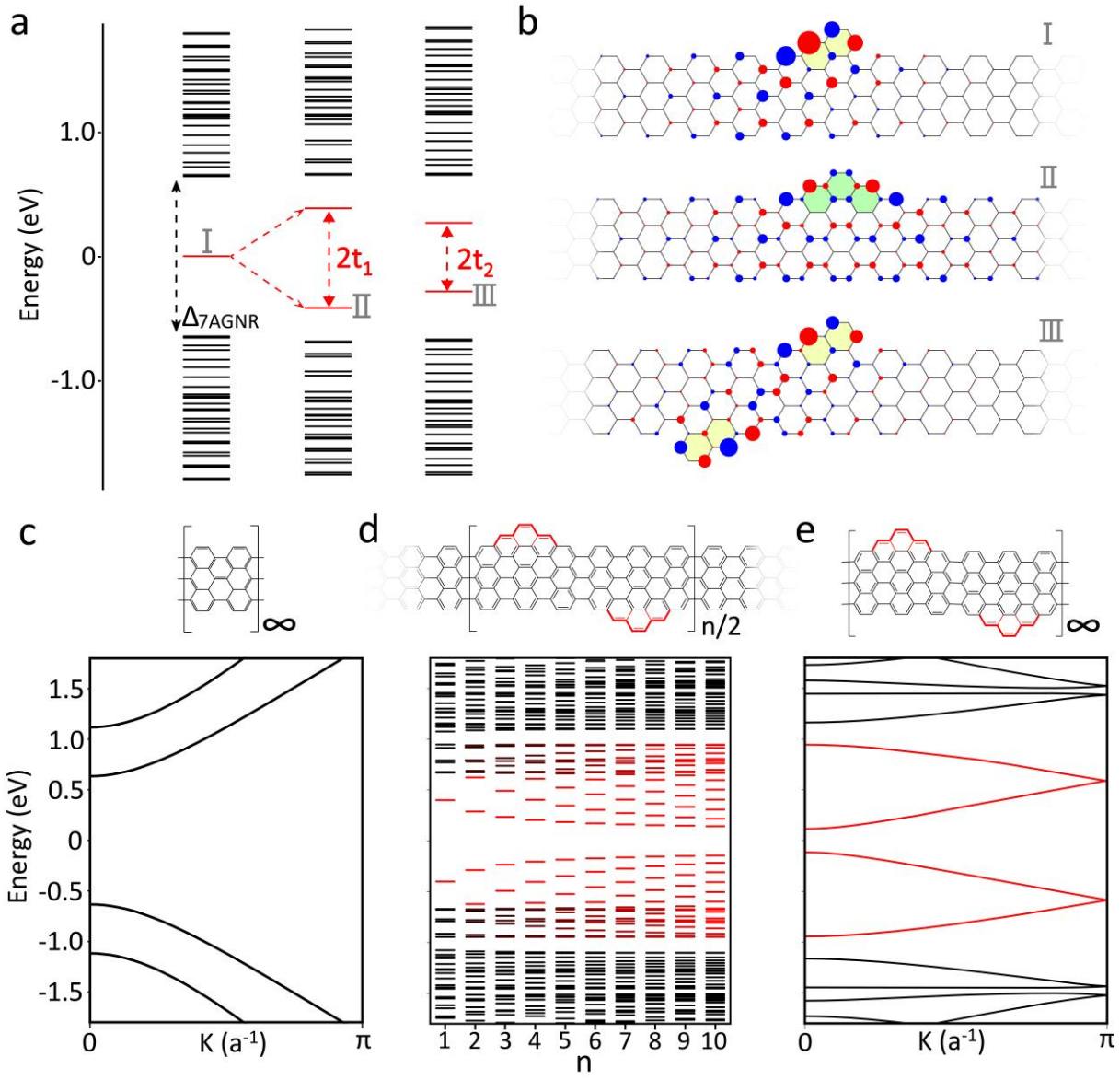

Figure 1. The tight-binding model of the edge extended graphene nanoribbons. a, The energy spectra of the edge extended 7AGNR with single topological junction (structure I in **b**) and two coupled topological junctions (structures II and III in **b**). The energy levels derived from the 7AGNR backbone are colored in black, while the topological in-gap state and hybridized states are inside the 7AGNR gap and colored in red. t_1 and t_2 reflect coupling strengths of the topological states in structure II and III, respectively. **b,** Structures I, II, III and their corresponding wave functions of the topological state of I and the HOMO of structure II

and III. The size of the circle represents the amplitude, and the color (red, blue) represents the parity of wave functions. **c,** The band structure of the pristine 7AGNR. **d,** The energy spectra of edge extended 7AGNR with different numbers of edge extensions (n) along the GNR backbone. The black energy levels originate from the 7AGNR, while the red ones are attributed to the topological bands. A gradual transition from black to red levels reflects the hybridization of the extensions with the pristine 7AGNR frontier bands. **e,** The band structure of 7-AGNR-S(1,3), while the red bands correspond to the topological bands.

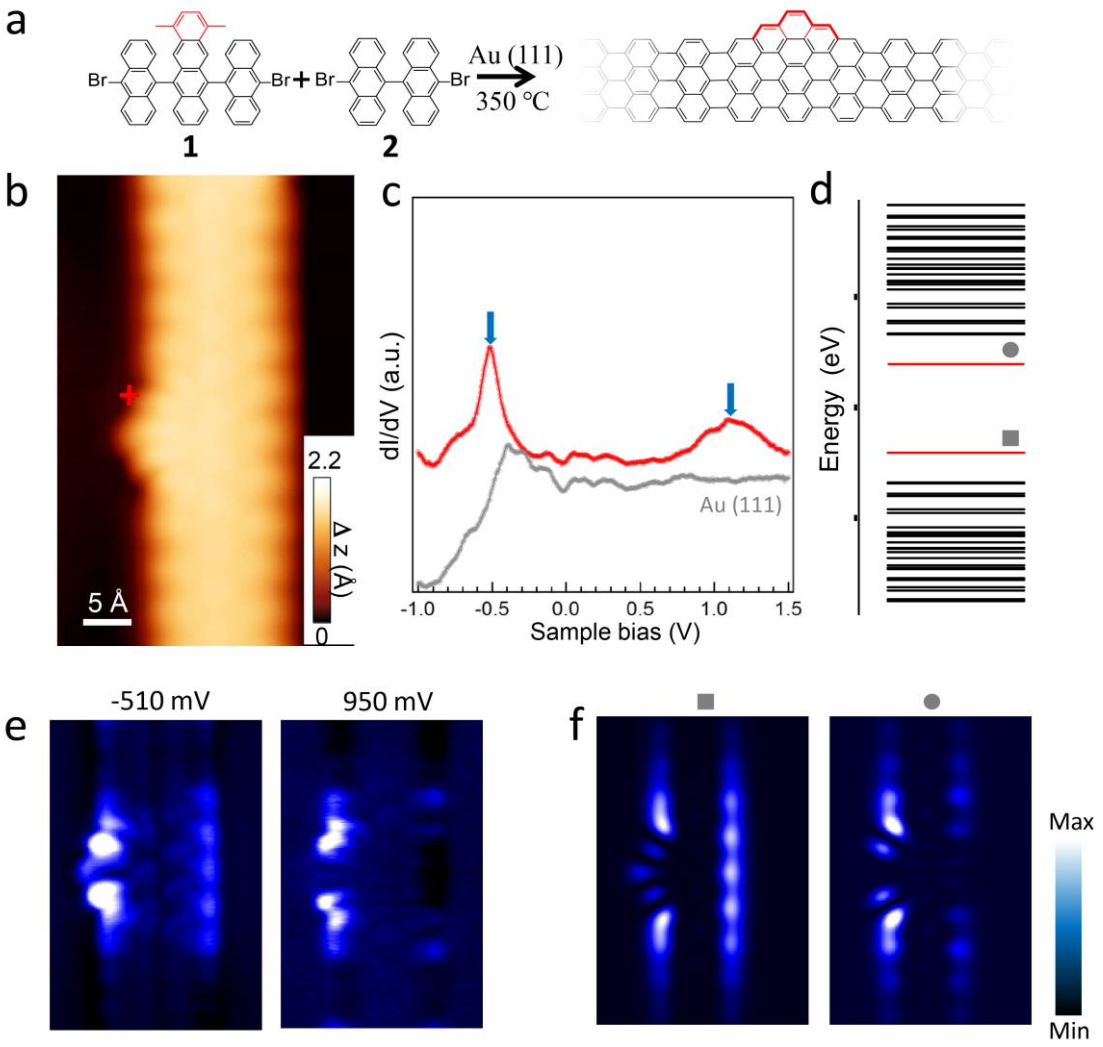

Figure 2. On-surface synthesis and characterization of the dimer structure II. a, The synthetic route to structure II from precursor molecules **1** and **2**. **b,** A typical STM image of structure II (V_s = -0.48 V, I_t = 400 pA). **c**, STS spectrum of the structure II with the acquisition position indicated in **b**. The arrows indicate HOMO and LUMO. The reference spectrum taken on the bare Au(111) is displayed in gray. **d,** TB calculated energy level of structure II with the topologically derived HOMO and LUMO colored in red. **e,** Constant-current STS maps of the topological HOMO and LUMO states. **f,** TB simulated LDOS maps of the HOMO and LUMO of which the energy levels are indicated by the corresponding symbols in **d**.

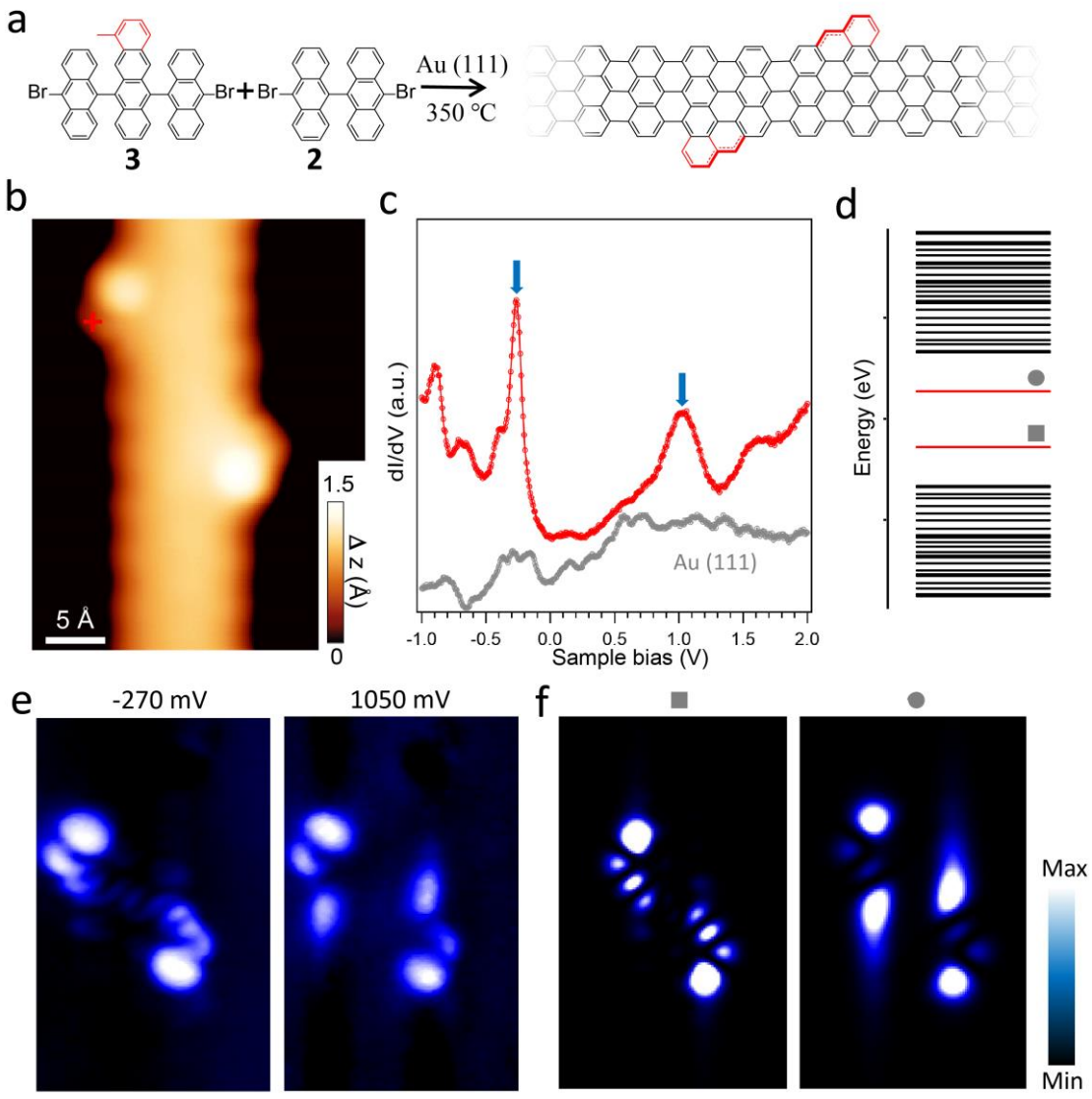

Figure 3. On-surface synthesis and characterization of the dimer structure III. a, The synthetic route to structure III from precursor molecules **3** and **2**. **b,** A typical STM image of structure III (V_s = 1.05 V, I_t = 500 pA). **c**, The STS spectrum of the structure III with the acquisition position indicated in **b**. The arrows denote HOMO and LUMO. The reference spectrum taken on the bare Au(111) is displayed in gray. **d,** TB calculated energy level of structure II with the topologically derived HOMO and LUMO colored in red. **e,** Constant-current STS maps of the topologically derived HOMO and LUMO. **f,** TB simulated LDOS maps of the HOMO and LUMO, of which the energy levels are indicated by the corresponding symbols in **d**.

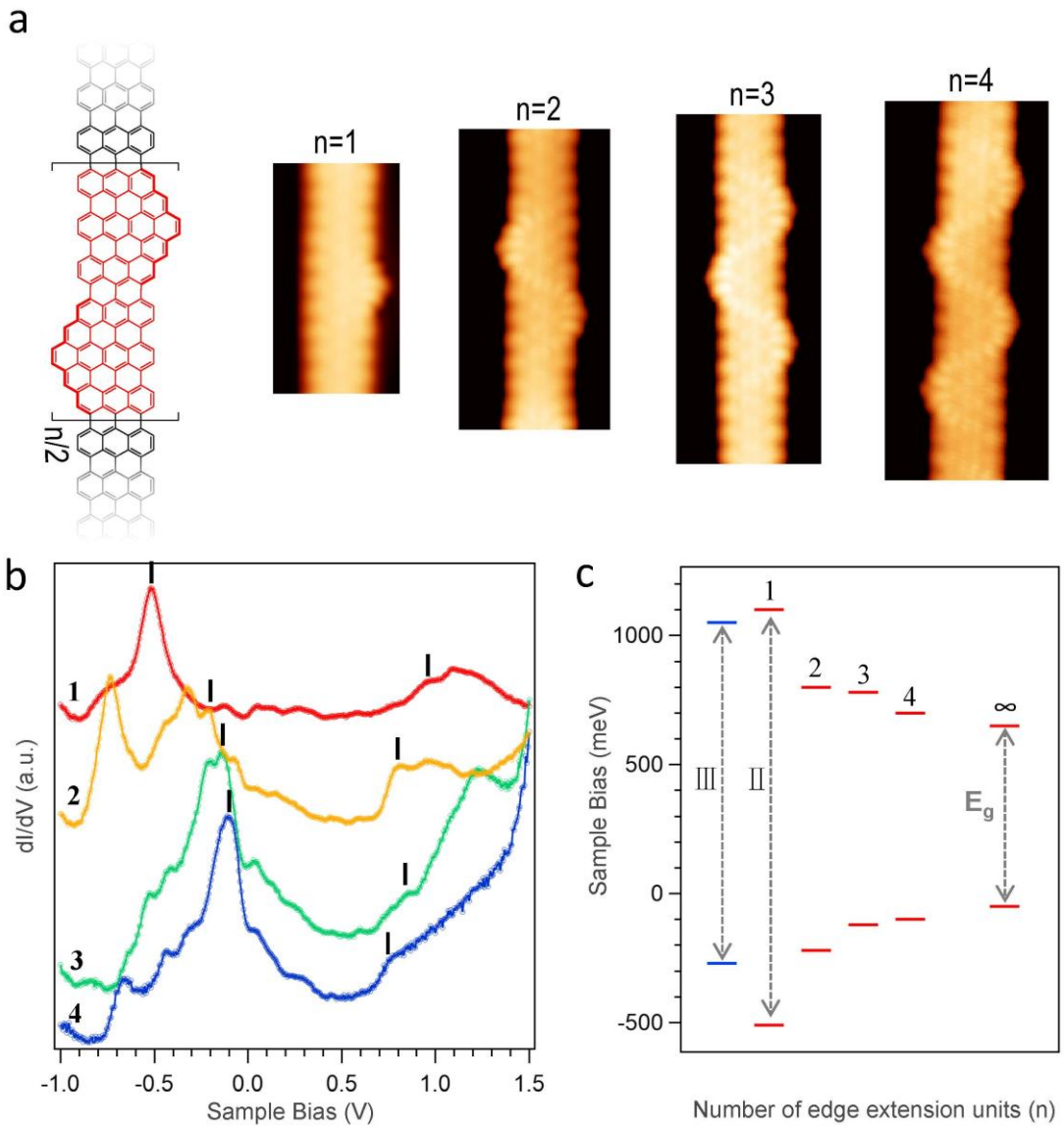

Figure 4. The electronic properties of GNRs with multiple edge extensions. a, The chemical sketch of edge extended GNRs. STM images of the GNR structures having one to four coupled edge extensions. **b,** The corresponding STS spectra of the structures in **a** showing the shrinking of the HOMO-LUMO gap with an increasing number of the extended edge. The HOMO/LUMO positions are indicated by vertical lines. The number indicates edge extension unit (n). **c,** The experimental determined frontier energy states as a function of the number of edge extension units (n). The energy positions of structure II and III are indicated, E_g represents the experimentally determined band gap of 7-AGNR-S(1,3) on Au(111).[11]